



# Solubility behaviour, crystallisation kinetics and pour point: A comparison of linear alkane and triacyl glyceride solute/solvent mixtures



Paul D.I. Fletcher<sup>\*</sup>, Noel A. Roberts, Choephel Urquhart

Surfactant & Colloid Group, Department of Chemistry, University of Hull, Hull HU6 7RX, UK

## ARTICLE INFO

### Article history:

Received 21 October 2015

Received in revised form 3 December 2015

Accepted 6 December 2015

Available online 14 December 2015

### Keywords:

Alkane  
Triacyl glyceride  
Solubility  
Crystallisation  
Pour point

## ABSTRACT

Mixtures of either a hydrocarbon wax in a hydrocarbon solvent or a long chain triacyl glyceride (TAG) in a TAG solvent show complex solubility boundary temperature hysteresis and precipitated crystal network formation leading to gelation. For these industrially-important systems, we show how the equilibrium solubility and its hysteresis, crystallisation kinetics and pour point temperature vary with solute concentration for representative examples of both hydrocarbon (*n*-tetracosane (C<sub>24</sub>) solute in *n*-heptane (C<sub>7</sub>) solvent) and TAG (tristearin (SSS) solute in tricaprilyn (CCC) solvent) mixtures. The behaviour is modelled with good accuracy; thereby providing a useful aid to formulation and process optimisation. © 2015 The Korean Society of Industrial and Engineering Chemistry. Published by Elsevier B.V. All rights reserved.

## Introduction

When a solution of either a long chain hydrocarbon wax in a short chain hydrocarbon solvent or a solution of a long chain triacyl glyceride (TAG) in a short chain TAG solvent is cooled, solute crystals are formed at temperatures below the solubility boundary temperature of the solution. Upon further cooling, sufficient crystals are produced to form a crystal network throughout the two-phase dispersion of crystals plus saturated solution. The crystal network causes gel formation and the mixture exhibits a finite yield stress and ceases to pour (flow) as a result of gravity [1–3]. The temperature at which this occurs is called the pour point temperature. Improving the understanding of the complex behaviour of these systems is important for many different technological applications. Failure of fuel and crude oils to flow caused by hydrocarbon wax crystallisation is a major problem for pipeline transport of crude oils and the use of hydrocarbon fuels in cold climates. Commercial products such as shoe polish consist of a semi-solid wax crystal network within a matrix of saturated solution. The processing of liquid TAG oil mixtures into semi-solid

fat products such as butter and margarine involves the precipitation of the high melting point TAG components, leading to the formation of a gelled fat crystal network which, in turn, determines many key properties of the final semi-solid fat product [4,5].

As a result of their industrial importance, there is extensive background literature on both hydrocarbon and TAG systems. For hydrocarbon systems, studies include measurement and modelling of equilibrium solubilities in alkane mixtures [6–21], alkane crystal nucleation and growth kinetics [22–25] and alkane crystal gel formation [1–3,26,27]. Relevant literature on TAG systems includes TAG polymorphism [28–30] and relation to solubility [31], TAG crystallisation (reviews [32–34] and specific TAG systems [35–40]) and fat crystal network and pour point properties [4,5,41]. Most practical applications involve systems containing either mixed hydrocarbon wax solutes in a mixed hydrocarbon solvent or mixed TAG solutes in a mixed TAG solvent. Despite the extensive literature, for both hydrocarbon and TAG systems, there is a lack of systematic investigation of the behaviour of single solute/single solvent mixtures which cover the entire solute concentration range. In particular, the following aspects are currently unclear.

- (i) How does the hysteresis between solubility boundary temperatures measured by heating ( $T_{\text{heat}}$ ) and cooling ( $T_{\text{cool}}$ )

<sup>\*</sup> Corresponding author. Tel.: +44 1482 465 433; fax: +44 1482 466 410.  
E-mail address: [P.D.Fletcher@hull.ac.uk](mailto:P.D.Fletcher@hull.ac.uk) (Paul D.I. Fletcher).

vary with solute concentration and how does this hysteresis relate to the kinetics of crystallisation?

- (ii) How does the pour point temperature (i.e. the temperature at which precipitated crystal network formation causes gelation of the system) vary with solute concentration and how does this relate to the curves of  $T_{\text{heat}}$  and  $T_{\text{cool}}$ ?
- (iii) Can we develop a self-consistent model to account for the solute concentration dependences of  $T_{\text{heat}}$ ,  $T_{\text{cool}}$  and the pour point temperature for both hydrocarbon and TAG systems?

Addressing questions (i)–(iii) for single solute/single solvent systems represents one step towards improving manufacturer's ability to rationally optimise processing conditions for the production of hydrocarbon and TAG systems involving precipitated crystal networks. We note here that extension to complex mixtures would be required for application in many systems of practical interest.

In order to tackle questions (i)–(iii) we have selected two solute/solvent systems which are representative of hydrocarbon and TAG systems of practical interest: *n*-tetracosane (abbreviated to C24) solute in *n*-heptane (abbreviated to C7) solvent and tristearin (abbreviated to SSS) solute in tricaprilyn (abbreviated to CCC) as solvent. For each system, we have measured and modelled the inter-linked properties of solubility and its hysteresis, crystallisation kinetics and pour point as functions of solute concentration and discuss the origins of the significant difference in observed behaviour between the hydrocarbon and TAG systems.

## Experimental

### Materials

*n*-Tetracosane (abbreviated to C24, Sigma-Aldrich, 99%), *n*-heptane (abbreviated to C7, Fischer Scientific, 99%), tristearin (abbreviated to SSS, Sigma-Aldrich, >99%) and tricaprilyn (abbreviated to CCC, Sigma-Aldrich, >99%) were used as received.

### Methods

Full details of the experimental methods used in the measurement of solubility boundary temperatures ( $T_{\text{heat}}$  and  $T_{\text{cool}}$ ), pour point temperatures and the extraction and imaging of precipitated crystals are given in Ref. [27]. Briefly, solubility boundary temperatures corresponding to the first appearance of crystal precipitates on cooling ( $T_{\text{cool}}$ ) or the maximum temperature at which crystal precipitates were present on heating ( $T_{\text{heat}}$ ) were determined by visual observation of the samples using a 5× magnification hand lens. Pour point temperatures were measured using a slightly modified version of the ASTM D97 procedure [42]. It was taken to be the highest temperature at which no flow of the sample was observed when the vessel was tilted from vertical to horizontal and found to be equal (within the experimental uncertainty of  $\pm 0.2^\circ\text{C}$ ) to the lowest temperature at which movement of the sample was observed on tilting. Solute crystals were extracted by rapid vacuum filtration, dried and sprinkled onto a carbon impregnated 'sticky disc' attached to a 15 mm diameter threaded Hitachi SEM mount. Crystal samples were imaged at various magnifications using a Hitachi TM-1000 SEM operating at 15 kV with a vacuum of 50 Pa.

Powder X-ray diffraction measurements were made using a PANalytical empyrean series 2 powder diffractometer. The X-ray source used is a Cu anode, with radiation wavelengths filtered using a single crystal germanium monochromator, emitting Cu  $K\alpha_1$  radiation (wavelength  $\lambda = 1.540593 \text{ \AA}$ ) at the samples. Circular sample holders were used, packed with the powdered material to be analysed. An automatic slit method was used,

measuring reflection intensity between angles of  $5^\circ$  and  $80^\circ$  over 15 min at controlled room temperature ( $25^\circ\text{C}$ ). Measured intensities were converted to relative intensities by dividing values by the peak diffracted intensity. The diffraction angle  $\theta$  scale values were converted to a crystal spacing scale according to spacing =  $\lambda / (2\sin(\theta/2))$ .

## Results and discussion

### Solubility as a function of temperature

Fig. 1 shows the variation of solubility boundary temperatures ( $T_{\text{heat}}$  and  $T_{\text{cool}}$ ) with solute mole fraction for both C24 in C7 and SSS in CCC. It can be seen that the C24/C7 shows a hysteresis in the solubility boundary temperatures (i.e. the difference between  $T_{\text{heat}}$  and  $T_{\text{cool}}$ ) of only 1–2  $^\circ\text{C}$  whereas the SSS/CCC has a much larger hysteresis of approximately 20  $^\circ\text{C}$ . As discussed in ref. [27], the process of melting of a precipitated crystal (as observed on heating at temperature  $T_{\text{heat}}$ ) is expected to have zero activation energy and so should occur promptly on increasing the temperature. Hence, the measured temperature  $T_{\text{heat}}$  is expected to correspond to the equilibrium solubility boundary temperature. In contrast, the process of crystal precipitation (observed on cooling at temperature  $T_{\text{cool}}$ ) is expected to occur by nucleation and growth and be subject to an activation energy barrier as described below. Hence, crystal precipitation does not occur promptly on cooling below the equilibrium solubility boundary; crystal formation on cooling is fast enough to be observed only when the system is undercooled to a temperature  $T_{\text{cool}}$  which is significantly below the equilibrium solubility boundary  $T_{\text{heat}}$ .

The simplest model to quantitatively predict the equilibrium solubility behaviour is based on the assumptions that the solute/solvent mixtures form ideal solutions (i.e. the volume and enthalpy

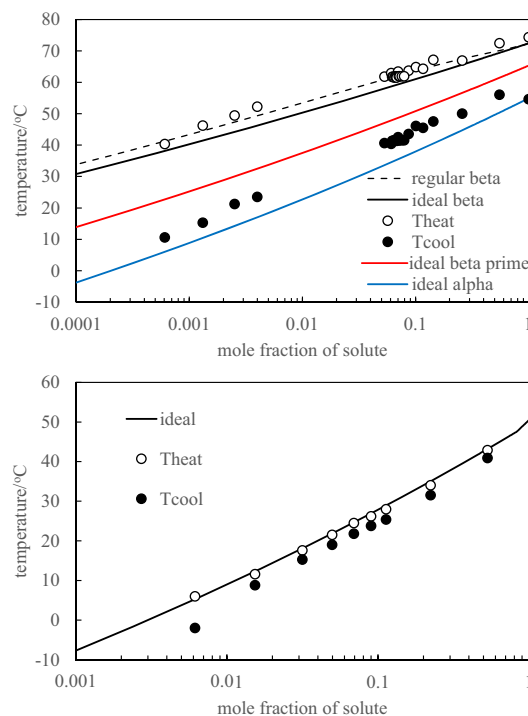


**Fig. 1.** Variation of solubility with temperature for SSS in CCC (upper plot) and C24 in C7 (lower plot). Solid curves are calculated according to ideal solution theory and the dashed curve corresponds to regular solution theory. For the SSS/CCC systems, calculated curves are shown for the  $\alpha$ ,  $\beta'$  and  $\beta$  polymorphs. For each plot, unfilled circles correspond to measured values of  $T_{\text{heat}}$  and filled circles show  $T_{\text{cool}}$  values.

Download English Version:

<https://daneshyari.com/en/article/228267>

Download Persian Version:

<https://daneshyari.com/article/228267>

[Daneshyari.com](https://daneshyari.com)